



Grey Signal Predictor and Fuzzy Controls for Active Vehicle Suspension Systems via Lyapunov Theory

T. Chen, C. C. Hung, Y. C. Huang, J. C. Y. Chen, Md. S. Rahman, Md. T. I. Mozumder

Tim Chen

Faculty of Information Technology
Ton Duc Thang University, Ho Chi Minh City, Vietnam
First author (Tim Chen): timchen@tdtu.edu.vn

Chih Ching Hung*

Department of Mechanical Engineering, National Taiwan University, Taipei, Taiwan
Faculty of Electronic Engineering, Taipei Municipal Muzha Vocational High School, Taipei, Taiwan
*Corresponding author: p9690110@gmail.com

Yu Ching Huang

Department of Earth Science, National Taiwan Normal University, Taipei, Taiwan
Center of Natural Science, Kaohsiung Municipal Fushan Junior High School, Kaohsiung, Taiwan

J. C. Y. Chen*

Department of Artificial Intelligence
University of Maryland, Maryland 20742, USA
*Corresponding author: jc343965@gmail.com, cjcy@umd.edu

Md. Samiur Rahman*

School of Engineering and Physical Sciences
North South University, Dhaka, Bangladesh
*Corresponding author: rahman.samiur07@gmail.com

Md. Towfiqul Islam Mozumder*

School of Engineering and Physical Sciences
North South University, Dhaka, Bangladesh
*Corresponding author: towfiqul.mozumder@gmail.com

Abstract

In order to investigate and decide that the vehicle asymptotic vibration stability and improved comfort, the present paper deals with a fuzzy neural network (NN) evolved bat algorithm (EBA) backstepping adaptive controller based on grey signal predictors. The Lyapunov theory and backstepping method is utilized to appraise the math nonlinearity in the active vehicle suspension as well as acquire the final simulation control law in order to track the suitable signal. The Discrete Grey Model DGM (2,1) have been thus used to acquire prospect movement of the suspension system, so that the command controller can prove the convergence and the stability of the entire formula through the Lyapunov-like lemma. The controller overspreads the application range of mechanical elastic vehicle wheel (MEVW) as well as lays a favorable theoretic foundation in adapting to new wheels.

Keywords: Evolved control, MEVW, Nonlinear Lyapunov method, Adaptive fuzzy control, artificial intelligence tool, Grey DGM (2,1) model.

1 Introduction

With the prompt development for the automobile industry, the security of automobiles has been remarkably improved. More and more car manufactures have begun to evaluate noise, vibration and irregularities [1, 2]. So far, a lot of work has been done to improve driving comfort, including the development of active steering, controlled steering and steering motors [3, 4]. As an indispensable part of a vehicle, suspension plays an important role of improving driving comfort as well as driving performance [5, 6, 7]. The key function is a focus to transfer power as well as torque between the road and the vehicle. Comparing with accustomed passive vehicle suspension, the active vehicle suspension is usually necessary to maintain the balance between vehicle characteristics, not merely to separate the vibration resulted from different driving environments, and it also to maintain favorable contact with roads [8]. Semi-active vehicle suspension and active vehicle suspension can alter the damping and stiffness coefficient at the same time. Although they require a lot of external power source to operate, they have the potential to enhance the overall performance in the vehicle and are therefore the most effective [9, 10, 11]. Many researchers have utilized it to evaluate active control of suspensions. Nowadays, the research of active vehicle suspension system control can be approximately differentiated into two categories: The first category includes intelligent control based on precise modeling, which mainly includes robust control, and optimal control, and neural networks, and adaptive control that could settle the nonlinear problems and enhance vehicle control manifestation. However, it should be pointed out that there is no completely known system model, and the intelligent control strategy is still a challenge. It is necessary to develop another control system which is known as a free model, and it does not rely on the system model. This control of the free model is expressed as unclear control when the system is adjusted and controlled based on the expertise and the experiences of experts [9, 20, 21, 22, 23], which was supported by predictive fuzzy technique with performances in parallel distributed control. Also, the robotic techniques with the distinct objects for the environment has been highlighted in the LMI and neuro-fuzzy modeling even for the applications in chaos and math nonlinearity. This scheme avoids tedious and inconvenient modeling labor and realizes the application for human knowledge, but it neglects the beneficial information in the system, and the accuracy is not often sufficient. Rather, modern active vehicle suspensions combine the benefits of these new types of control (for example, adaptive control) with conventional control strategy. This scheme uses reverse thought to estimate problems and uses adaptive schemes to solve unknown factors of a particular system. Control laws are easier to understand and adapt with the adaptive rollback control strategy. Active vehicle suspension can solve difficult limitations [24], and most existing active vehicle suspension systems are utilized with conventional pneumatic wheels. Simplified stiffness and damping are utilized to replace the wheel without pondering the actual performance for the wheel. The algorithm might be easy, but it is far from reality. These neural systems are composed of simple compositions working in parallel. Those compositions are inspired via sensory natural systems. Therefore, the network is utilized to approximate the nonlinear frame, making it as close as possible to the neural network (NN). In order to simplify the control problem, these LDI connections (using differential linear inclusion) is utilized in the present paper to control the stability in a large nonlinear frame. The Evolved Bat Algorithm (EBA) was developed, which is known to be suitable for solving optimization numerical problems for swarm intelligence.

Simultaneously, a new type of mechanical elastic vehicle wheel (MEVW) has been developed, which has the benefits of being explosion-proof as well as light weight, and have attracted widespread attention. Relevant studies have shown the performances with artificial intelligence tools [25, 26, 27, 28]. The accustomed control strategy is difficult to adapt to the vehicle suspension system prepared with MEVW. Although these vehicle wheels are mounted in an active vehicle suspension, their high radial strength also make it difficult to guarantee the performance. Generally, work on control strategies for improving vehicle comfort on such wheels (especially active vehicle suspensions) is rarely factualized on control strategies. It is necessary to consider the non-linear system and perform certain operations in this area with certainty. Although great efforts have been made for nonlinear and non-safety systems such as adaptive control, and sliding control, and fuzzy control, as well as grey system methods, it is always necessary to take into account the math nonlinearity and uncertainty to reflect the sensor's actual movement. This makes it difficult to implement control strategies. According to the model's

predictive control idea, we can control whether the prospect conditions can be met in advance. Accustomed forecasting methods take these factors into account, which is a major problem [29, 30, 31, 32]. These include statistical regression, and Holt-Winters method, and ARMA model [33, 34]; however, these are not simple to apply to actual technologies. Gray's system theory rarely uses information about data to find mathematical relationships between factors and then predict them. The DGM gray model (2.1) is particularly adequate for depicting non-monotonic vibration sequences and is widely utilized in signal vibration processing [35, 36]. Therefore, this study uses the gray DTM model (2.1) to provide predictive information that the controller could make the best or most effective use for the vehicle suspension system. Shortly speaking, the key content in the article is to put forward a new type of mechanically elastic wheels to guard against tire explosions, and to devise effective control measures to equip these new wheels with active vehicle suspension. By using evolved bat algorithm combined fuzzy theory, the control system can be approximated more effectively and efficiently. Unlike the rest intelligent swarm algorithms, the advantage of the EBA combined fuzzy theory has one measurable factor (called an intermediate parameter) which needs to be determined. The choice of another medium judges the scale of the research steps in the evolutive process. In order to report the actual situation, the present study evaluated the non-linearity and uncertainty of the wheels and suspension. With this in mind, Taylor series are utilized to enlarge the nonlinear utterances of damping force and spring force under unknown measurable factors. Thus, we use adaptive recoil control and Lyapunov theory to reckon these unknown measurable factors and tail the ideal spring motion for better performance. Taking into account the additional correlation of these ideal vehicle suspension motions, the gray signal predictor is utilized to design prospect vehicle suspension motion. Lastly, the simulation of the numerical results verify the reliability as well as effectiveness for the control method proposed in the study. The rests in this article are organized as the following. The description in the system is given in the second part. The existence of the modeling errors provides sufficient conditions for nonlinear systems and guarantees partial asymptotic vibration stability in section III. Examples with simulation calculations explain the possibilities of our method of section IV, and some speculating observations at the end of the paper.

2 System Description

As shown in Figure 1 (a) and (b), the mechanical elastic vehicle wheel (MEVW) is primarily constituted by an elastic wheel (wire loop, rubber layer), a hinge and a hub group. The elastic wheel is composed of a metal ring as well as a rubber layer. For simplicity, Figure 1(c) shows that when the length l of the hinge group is slightly larger than the unloaded length, the hinge allows a certain degree of radial motion; however, whilst the MEVW is loaded, these loads on the wheel will pass by the hinge group. These distances between the spring wheel and the hub could be called the free movement in the hinge group. The bottom is obviously deformed, and the top tends to shrink radially. Due

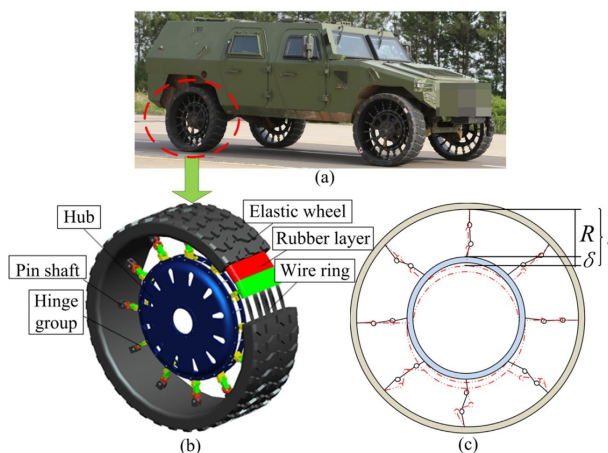


Figure 1: MEVW system.

to this structure, the joint group has only one pulling force. The MEVW has been tested to achieve these characteristics, and the load has been increased from 0 kN to 20 kN. Figures 2(a) and 2(b) show the test equipment and results for 2 kN step and vertical strain, respectively. Figure 2(b) shows the vertical deformation (about 3mm) of the MEVW during unloading. The main reason is MEVW is influenced by gravity force, and the hub could move smoothly for certain distances. Upon these hinge groups were extended to its maximum extent, a load was employed and these wheels began to support those weights. The stiffness characteristic in MEVW is evidently not linear. The active vehicle suspension is equipped with mechanical elastic vehicle wheels, and the half-car model has been utilized to depict these systems. The damping forces are considered to be non-linear and unknown numbers. The systems measurable factors were listed in Table 1.

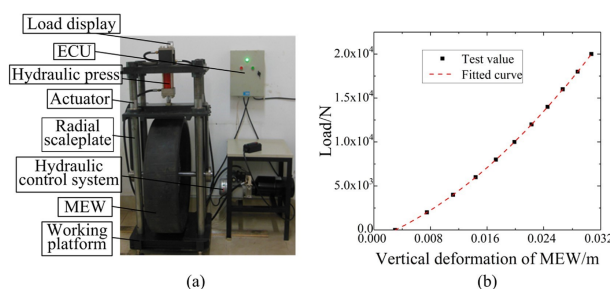


Figure 2: Relationship between deformation and load of MEVW.

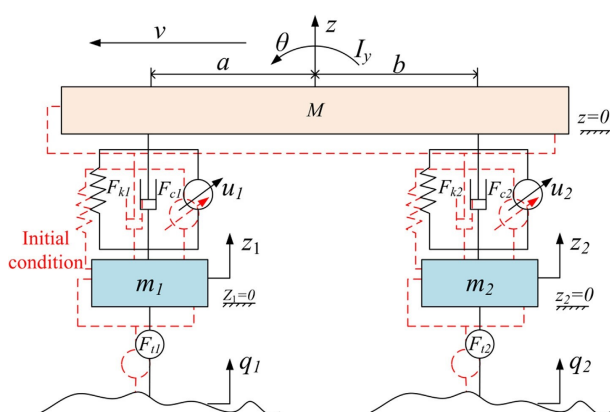


Figure 3: Active vehicle suspension and MEVW control model.

Table 1 Nomenclature.

Symbol	Description
M	Mass of car body
m_1, m_2	Mass of front or rear MEW
z	Vertical displacement of car body
z_1, z_2	Vertical displacement of front or rear MEW
I_y	Moment of inertia around the centroid
h	Pitch angle of car body
a, b	Distances between centroid and front or rear suspensions
F_{k1}, F_{k2}	Spring force of front or rear suspension
F_{c1}, F_{c2}	Damping force of front or rear suspension
u_1, u_2	Forces generated by front or rear actuator
F_{t1}, F_{t2}	Tire forces of front or rear MEW
v	Speed of vehicle
q^1, q^2	Road profiles

The initial condition is determined in these positions in which there is no force for the vehicle

suspension and tire. The orientation of the axis is shown as seen in Figure 4. These dynamics could be depicted as the following [37]:

$$\begin{cases} \dot{x}_1 = x_2 \\ \dot{x}_2 = \frac{1}{M}[-F_{k1} - F_{c1} + u_1 - F_{k2} - F_{c2} + u_2 - Mg] \\ \dot{x}_3 = x_4 \\ \dot{x}_4 = \frac{1}{I_y}[F_{k1}a + F_{c1}a - u_1a - F_{k2}b - F_{c2}b + u_2b] \\ \dot{x}_5 = x_6 \\ \dot{x}_6 = \frac{1}{m_1}[F_{k1} + F_{c1} - u_1 + F_{t1} - m_1g] \\ \dot{x}_7 = x_8 \\ \dot{x}_8 = \frac{1}{m_2}[F_{k2} + F_{c2} - u_2 + F_{t2} - m_2g] \end{cases} \quad (1)$$

The wide practical usage of the theoretic results presented for the math nonlinearity of vehicle suspension and MEVW has been evaluated, and the active vehicle suspension system prepared with MEVW is modeled. The vehicle suspension force as well as tensile strength of MEVW have been expressed through experimental analysis and Taylor series. In the next part, we will study the design of an active landing gear controller that conforms to the MEVW. Vehicle suspension system control comprises ideal vehicle suspension motion generator, adaptive feedback control law, and gray signal predictor. The signal controls the movement of the vehicle suspension to follow ideal conditions, and the signal predictor predicts the required conditions based on the pre-regulated control law. The control structure is shown in Figure 4. To stabilize the car fuselage, the present study assumes that there is an ideal x_{1d} and x_{3d} vehicle suspension motion. While the vertical actual movement as well as inclination (x_1, x_3) in the vehicle could detect the required movements, driving comfort could be warranted. First, let us stint the tracking errors.

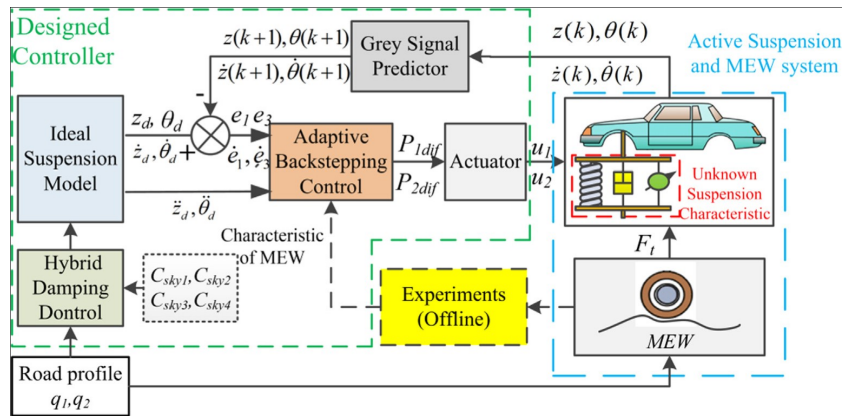


Figure 4: The design of controller in active vehicle suspension and MEVW.

It is necessary to introduce Lyapunov's positive definite function (PD) for the system state so that the tracking error gradually approaches zero when the derivative is considered as negative definite (ND). This has the chosen function.

$$\begin{aligned} \dot{V}(e_1, e_3, \delta_2, \delta_4) &= e_1\dot{e}_1 + e_3\dot{e}_3 + \delta_2\dot{\delta}_2 + \delta_4\dot{\delta}_4 \\ &= e_1(\dot{x}_{1d} - x_2) + e_3(\dot{x}_{3d} - x_4) + \delta_2\dot{\delta}_2 + \delta_4\dot{\delta}_4 \\ &= e_1[\dot{x}_{1d} - (\dot{x}_{1d} + k_1e_1 - \delta_2)] + e_3[\dot{x}_{3d} - (\dot{x}_{3d} + k_3e_3 - \delta_4)] + \delta_2\dot{\delta}_2 + \delta_4\dot{\delta}_4 \\ &= -k_1e_1^2 - k_3e_3^2 + \delta_2(e_1 + \dot{\delta}_2) + \delta_4(e_3 + \dot{\delta}_4) \end{aligned} \quad (2)$$

According to Lyapunov’s ND theory, for ND of equation (2), the tracking error and the estimation error tend to zero. So, it is essential to present a definite positive Lyapunov function (PD) which is related to the state to make it function step by step. If the derivative of the negative definite (ND) is zero, it is the selected to function. Theoretically, this shows the possibility of control and the convergence of tracking the errors. This completes the control signal and estimated measurable factors of the active vehicle suspension according to the MEVW and general controlling law.

To actually give birth the necessary force of the vehicle, a hydraulic vehicle suspension was selected. The generator of this system is composed in actuator, hydraulic source as well as hydraulic electro servo valve. These pressure differences between these two are very large as illustrated in Figure 5. Both positions of the piston for the actuator are diametrically controlled via the hydraulic electro servo valve. These oil hydraulic flows through the actuator as well as the flows generate forces for the piston owing to these differences in tension. The resulting forces could then be counted. The above strategy was designated to cause the vehicle suspension guide an ideal movement for accommodating suspensions in difference. The following is an ideal sports layout. An ameliorated damping hybrid control is provided that combines ground hook and cloud hook damping control to provide the desired motion as indicated in Figure 6.

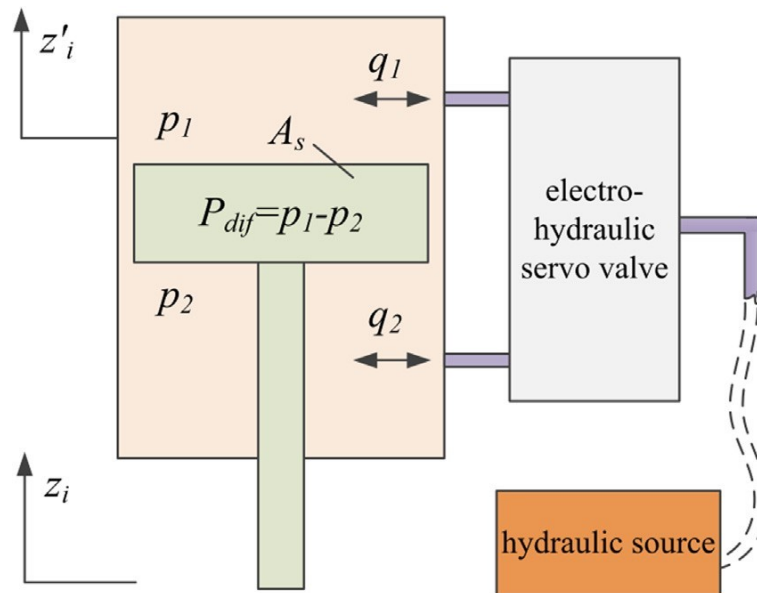


Figure 5: The mechanism for the actuator.

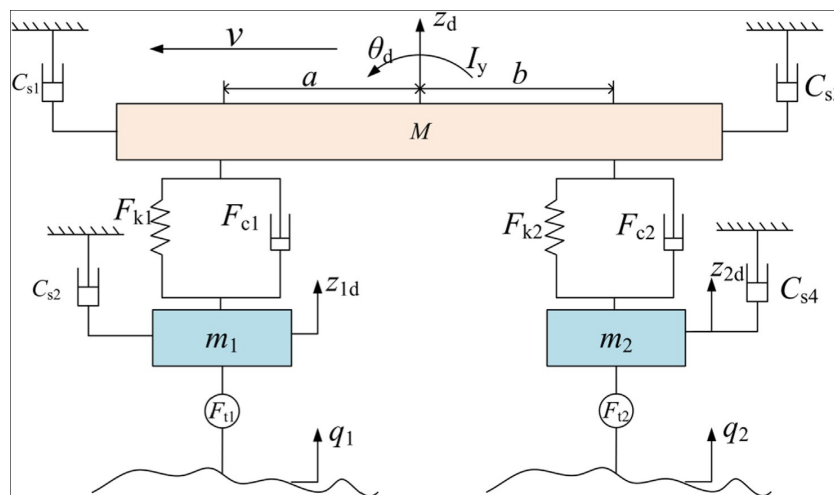


Figure 6: Damping hybrid mechanism to track the ideal movement.

To consider the NN model, S-layers by $R^q (q = 1, 2, \dots, S)$ neurons in each layer, where $x(k) \sim x(k - m + 1)$ is state math variables as well as $u(k) \sim u(k - n + 1)$ input math variables. These numbers in the layer are subjoined as an inscription to the denominations for the variables. So, the weighted matrix in the qth layer would be written as W^q . Then the final output in the NN model could be referred to as follows:

$$x(k + 1) = \Psi^S (W^S \times \Psi^{S-1} (W^{S-1} \times \Psi^{S-2} (\dots \Psi^2 (W^2 \times \Psi^1 (W^1 \times Z(k))) \dots))) \tag{3}$$

In addition, according to the interpolation equation and method, the present study can acquire

$$\begin{aligned} x(k + 1) &= \left\{ \sum_{j_1^S=1}^2 \dots \sum_{j_{r^S}=1}^2 h_{j_1^S}^S(k) \dots h_{j_{r^S}}^S(k) G(v^S, \Psi^S) (W^S \times [\dots [\sum_{j_1^2=1}^2 \dots \sum_{j_{r^2}=1}^2 h_{j_1^2}^2(k) \dots h_{j_{r^2}}^2(k) \right. \\ &\quad \cdot G(v^2, \Psi^2) (W^2 \times [\sum_{j_1^1=1}^2 \dots \sum_{j_{r^1}=1}^2 h_{j_1^1}^1(k) \dots h_{j_{r^1}}^1(k) G(v^1, \Psi^1) (W^1 \times Z(k))] \dots]) \left. \right\} \\ &= \sum_{v^S} \dots \sum_v h_{v^S}^S(k) \dots h_v^1(k) G(v^S, \Psi^S) W^S \dots G(v^1, \Psi^1) W^1 Z(k) \\ &= \sum_v h_v(k) J_v(W, \Psi) Z(k), \end{aligned} \tag{4}$$

The dynamics in the NN model could be rewritten by the passing LDI representation:

$$x(k + 1) = \sum_{i=1}^{\phi} h_i(k) J_i Z(k) = \sum_{i=1}^{\phi} h_i(k) \{A_i x(k) + B_i u(k)\}, \tag{5}$$

and J_i is a constant matrix with the appropriate dimension associated with $J_v(W, \psi)$. In addition, A_i and B_i are called partitions of J_i which is relevant to these partition $Z(k)^T = [x(k) \dots x(k - m + 1) u(k) \dots u(k - n + 1)]$.

Herein, a model-based fuzzy controller is synthesized to stabilize the discrete-time nonlinear system.

IF $x_1(k)$ is M_{i1} and ... and $x_m(k)$ is M_{im} THEN $u(k) = k_i x(k), i = 1, 2, \dots, l$ (6(a))

where l is the number of IF-THEN rules; and $M_{ij} (j = 1, 2, \dots, m)$ are the fuzzy sets.

The final amount produced in this fuzzy controller is deduced as the following:

$$\begin{aligned} u(k) &= - \frac{\sum_{j=1}^J w_j(k) K_j x(k)}{\sum_{j=1}^{J_i} w_j(k)} = - \sum_{j=1}^{J_i} \bar{h}_j(k) K_j x(k), \\ \text{with } w_j(k) &= \prod_{\mu=1}^p M_{j\mu}(x_{\mu}(k)), \quad \bar{h}_j(k) = \frac{w_j(k)}{\sum_{j=1}^{J_i} w_j(k)} \end{aligned} \tag{6(b)}$$

where $M_{j\mu}(x_\mu(k))$ is the rank of membership in $x_\mu(k)$ of $M_{j\mu}$. In this present study, it has been also supposed that $w_{j(k)} \geq 0$ as well as in all $\sum_{j=1}^{J_l} w_{jl}(k) > 0$. So, $\bar{h}_j \geq 0$ as well as of all $\sum_{j=1}^{J_l} \bar{h}_j = 1$ of all k .

3 Evolved NN modeling and Stability of Grey signal predictor

The desired ideal motion can be achieved through improved hybrid damping control. Note that the hybrid attenuator is virtual, in fact, there is no need to design controls in practice, and the virtual attenuation coefficient is given as a control signal. Compliance with control laws include error and price tracking. In other words, it is ideal, and a true vehicle suspension with speed. It can design the suitable signal. Only real signal $x_1; x_2; x_3$; can predict x_3 beforehand to even more improve driving comfort. These DGM models (2.1) in gray system statement is utilized to devise predictors according to little-known material (at least 4), in which the present study can be easily implemented on a microcomputer. Assuming the number is n , this is a partialized motion sequence. When $B = [p, q]$, the DGM model (2, 1) can be depicted as follows.

$$\alpha^{(1)}x^{(0)}(k) + px^{(0)}(k) = q, \quad Bh = Y$$

$$B = \begin{bmatrix} -x^{(0)}(2) & 1 \\ -x^{(0)}(3) & 1 \\ \vdots & \vdots \\ -x^{(0)}(n) & 1 \end{bmatrix}, Y = \begin{bmatrix} \alpha^{(1)}x^{(0)}(2) \\ \alpha^{(1)}x^{(0)}(3) \\ \vdots \\ \alpha^{(1)}x^{(0)}(n) \end{bmatrix} = \begin{bmatrix} x^{(0)}(2) - x^{(0)}(1) \\ x^{(0)}(3) - x^{(0)}(2) \\ \vdots \\ x^{(0)}(n) - x^{(0)}(n-1) \end{bmatrix} \tag{7}$$

After the prediction is completed, the actual value of the signal will be measured at the appropriate time. Since the movement of the vehicle suspension is strongly influenced by stochastic excitation, they are difficult to guarantee sheer accuracy. While comparing these predicted amounts for the actual value, upon the error has been acceptable, these errors are sent, on the contrary, another actual signal are sent. Please note that these short-term status signals would not alter significantly. So, as shown in the equation, 5 times the sheer differences between the previous signals and current signals are sets whilst the error threshold are indicated in Equation (8).

$$\hat{x}^{(0)}(n+1) = \begin{cases} \hat{x}^{(0)}(n+1) & \left| \hat{x}^{(0)}(n+1) - x^{(0)}(n) \right| \leq 5|x^{(0)}(n) - x^{(0)}(n-1)| \\ x^{(0)}(n) & \left| \hat{x}^{(0)}(n+1) - x^{(0)}(n) \right| > 5|x^{(0)}(n) - x^{(0)}(n-1)| \end{cases} \tag{8}$$

Next prediction of vehicle suspension motions $x_1, \hat{x}_1, x_3, \hat{x}_3$ add the measured value $x^{(0)}(n+1)$ to the deletes $x^{(0)}(1)$ and final stage of the numerical sequence $x^{(0)}$ (the distant right of the line vector) to respectively yield a new numerical sequence, iterating the higher level steps for accomplishing these metabolisms in grey DGM (2,1) model. Based on the dynamics of the NN model (5) with controllers,

$$x(k+1) = \sum_{i=1}^n \sum_{j=1}^J \bar{h}_j(k) h_i(k) H_{ij} x(k) + e(k)$$

where $H_{ij} = A_i - B_j K_j$, $\Re(x(k)) \equiv f(x(k), u(k))$, $e(k) = [\Re(x(k)) - \sum_{i=1}^{r_i} \sum_{j=1}^J h_i(k) \bar{h}_j(k) H_{ij} x(k)]$

and $e(k)$ represents the simulation error between the NN model and its nonlinear system. If there is

a definite and positive matrix P and there is a positive parameter k subsist such that the inequalities are as follows:

$$H_{ij}^T P H_{ij} - P < 0, \quad (1 + \kappa) H_{ij}^T P H_{ij} - P + (1 + \kappa^{-1}) \lambda_{\max}(P) H_q^T H_q < 0 \tag{9}$$

are satisfied for $j = 1, 2, \dots, l; i = 1, 2, \dots, \phi$ in which the $\lambda_{\max}(P)$ denotes those maximum eigenvalues in P , the nonlinear system is thus asymptotically stable. Proof: in Appendix. The Evolved Bat Algorithm (EBA) has been put forward on the basis of the bat echolocation system, which is worth pointing out in nature [38, 39, 40]. Unlike other intelligent swarm algorithms, the advantage of the EBA is that before using the algorithm to solve a problem, only one measurable factor (called an intermediate parameter) needs to be determined. The choice of another medium determines the scale of the research steps in the evolutionary process. This present study choses to air as a medium because they are in the middle of origin is the presence in its live bat. The function of EBA could be indicated into four short steps [41, 42]:

a. Initialization Step: These artificial agents are disseminated into the response space by stochastically assigning coordinates to them.

b. Movement Step: The artificial agents are moved. A stochastic number is generated and then it is checked if it is larger than the fixed pulse emission rate. If the result is positive, the artificial agent is moved using the stochastic walk process $x_i^t = x_i^{t-1} + D$, where x_i^t signifies the math coordinate in the i -th artificial agent for the t -th iteration; signifies the math coordinate in the i -th artificial agent for the last iteration; and D is the distance which the artificial agent shifts in this repetition. Thus, $D = \lambda \Delta T$, in which λ a state of affairs that does not change corresponding to the medium given of the experiment; and $\Delta T \in [-1, 1]$ is a random number. $\lambda = 0.17$ is utilized in our experiment because the chosen medium is air. $x_i^{tR} = \beta(x_{best} - x_i^t)$, $\beta \in [0, 1]$, in which β a random number; x_{best} signifies the math coordinate in the near best solution found so far in all places for all artificial agents; and x_i^{tR} signifies the new math coordinates in the artificial agent after these actions in these stochastic walk processes.

c. Evaluation Step: These fitness in the artificial agents have been counted by the updated to the stored and user stinted fitness function near best solution.

d. Termination Step: The abrogation conditions are determined for deciding whether to go backwards into Step b or repeal output and the program the near best solution. The appraisal criterion in order to determine the fitness in a bat has been judged a user stinted fitness numerical function. A fitness numerical function has been introduced in the present paper to find the control force of the controller and the collaborative positive symmetric definite matrix. Generally, intelligent swarm algorithms require multiple numerical iterations for finding the next best solution. Therefore, the same numerical experiment must be iterated some times to guarantee that the convergence is in numerical results and they are consistent. For the choice of air medium material, because it adapts to environments where bats live. The total size represents the number in artificial averages at the same time utilized in the numerical solution area for each numerical iteration. The present study defined the global scale as well as these numbers in possible solution so that they are sufficient to determine the complex system measurable factors that are not yet clear in the application.

4 Example

If the time step is small enough, all states of the system are continuous functions of time. The steps in DGM (2.1) should make the control stable and restricted. The controller is adapted to the condition of receiving the gray signal of the predictor, and has adaptive recoil force control to follow the motion generated by the ideal hybrid damping control to stabilize the motion of the MEVW equipped with active vehicle suspension. To the control circuit controls the first check a DGM (2.1) is correct, to simulate a numerical set of stochastic motion data using these trailers, the predicted signal numerical sequence number 6 is set to 0.001 seconds, and Simulink the up step is then designed two A standard tunnel (pulse and step) to demonstrate the effectiveness for the proposed control. These

road links acting in the rear and facade wheels have certain time lag, which are corresponding to the vehicle speed and wheelbase. The simulation measurable factors are shown in Table 2. It can be seen from the figure. It could be seen in Figure 7 in which these differences between the prediction (2, 1) of the GDM model and the accurate data is very small, especially when the trend is relatively small. If the data changes significantly, the tracking error in the GDM model (2.1) will be slightly larger; however, it can meet the requirements for engineering work. So, the the quality of being trustworthy in DGM (2.1) can be assured. The weighted matrices in the output and the hidden layer have been represented via W^2 and W^1 . After we train via the BP algorithm, the weighted factor could be acquired in Equations as follows.

$$v_r^1 = W_{1r}^1 x(k) + W_{2r}^1 x(k-1) + W_{3r}^1 u(k), \quad v_1^2 = W_{11}^2 T(v_1^1) + W_{21}^2 T(v_2^1) + W_{31}^2 T(v_3^1), \quad x(1+k) = T(v_1^2)$$

$$x(1+k) = (h_{11}^2(k)g_1 + h_{12}^2(k)g_2)v_1^2 = \sum_{i=1}^2 h_{1i}^2(k)g_i v_1^2. \tag{10}$$

Moreover, based on renumbering these matrices, the NN model then could be alternated into LDI representation as follows:

$$x(1+k) = \sum_{i=1}^{16} h_i(k) \{A_i x(k) + B_i u(k)\} \tag{11}$$

where

$$A_1 = A_2 = \dots = A_9 = \begin{bmatrix} 0 & 0 \\ 1 & 0 \end{bmatrix}, \quad A_{10} = \begin{bmatrix} -0.0598 & -0.2443 \\ 1 & 0 \end{bmatrix}, \quad A_{11} = \begin{bmatrix} 0.0148 & -0.0214 \\ 1 & 0 \end{bmatrix},$$

$$A_{12} = \begin{bmatrix} 0.1266 & -0.0039 \\ 1 & 0 \end{bmatrix}, \quad A_{13} = \begin{bmatrix} -0.0451 & -0.2657 \\ 1 & 0 \end{bmatrix}, \quad A_{14} = \begin{bmatrix} 0.0668 & -0.2482 \\ 1 & 0 \end{bmatrix},$$

$$A_{15} = \begin{bmatrix} 0.1414 & -0.0252 \\ 1 & 0 \end{bmatrix}, \quad A_{16} = \begin{bmatrix} 0.0816 & -1.2695 \\ 1 & 0 \end{bmatrix},$$

$$B_1 = B_2 = \dots = B_9 = \begin{bmatrix} 0 \\ 0 \end{bmatrix}, \quad B_{10} = \begin{bmatrix} -0.1172 \\ 0 \end{bmatrix}, \quad B_{11} = \begin{bmatrix} 0.0266 \\ 0 \end{bmatrix}, \quad B_{12} = \begin{bmatrix} -0.0120 \\ 0 \end{bmatrix},$$

$$B_{13} = \begin{bmatrix} -0.0906 \\ 0 \end{bmatrix}, \quad B_{14} = \begin{bmatrix} -0.1292 \\ 0 \end{bmatrix}, \quad B_{15} = \begin{bmatrix} 0.0147 \\ 0 \end{bmatrix}, \quad B_{16} = \begin{bmatrix} -0.1025 \\ 0 \end{bmatrix}. \tag{12}$$

The pitch curve is given in Figure 8 (a). After 1 second, a next signal step by a 0.1 m amplitude is displayed, and then the street height remains constant. The reaction to the active vehicle suspension containing MEVW was observed throughout the process.

It can be seen from the figure. It could be observed in Figure 8(b) that during these pulling, the active vehicle suspension system control force is displayed for 1 second. The maximum control force of the front vehicle suspension has 11490 N, as well as these rear control forces decreases after around 30 minutes. 0.3 seconds to reach 14.790N. After a period of time, the vehicle stabilizes again and the actuator control force is zero. Figures 8 (c) as well as 8(d) depict the vertical vibration displacement and upward movement of the body during stepping in. The adaptive recoil control scheme without or with the gray signal predictor could result in the active vehicle suspension system by MEVW follow the devised ideal motion well, while compared with the situation without control (> 3s), it can Make the vehicle more stable (< 1.5) s.

Although the efficiency of the adaptive regression control using the gray signal predictor has been better than that of the accustomed predictor, the amplitude of the vertical movement of the vehicle

in maximum is stifled by 7.44%, as well as the upward movement is reduced by 19% and 7%. In the case of a gray signal predictor, the controlled motion range is smaller than that without a gray signal predictor.

Table 2 program measurable factors.

Parameters	Values	Unites	I	Parameters	Values	Unites
M	730	kg		a21	19,600	N*m
I _y	1230	kg*m ²		a22	1	N*m ²
m ₁	40	kg		a23	1	N*m ³
m ₂	40	kg		b21	1290	N*s*m ¹
g	9.8	m*s ²		b22	1	N*s ² *m ²
a	1.1	m		b23	1	N*s ³ *m ³
b	1.8	m		d	0.003	M
v	10	m*s ¹		C _{sky1}	2000	N*s*m ¹
a11	19,600	N*m ¹		C _{sky2}	2000	N*s*m ¹
a12	1	N*m ²		C _{sky3}	2000	N*s*m ¹
a13	1	N*m ³		C _{sky4}	2000	N*s*m ¹
b11	1290	N*s*m ¹		k ₁	10	-
b12	1	N*s ² *m ²		k ₂	10	-
b13	1	N*s ³ *m ³		-	-	-

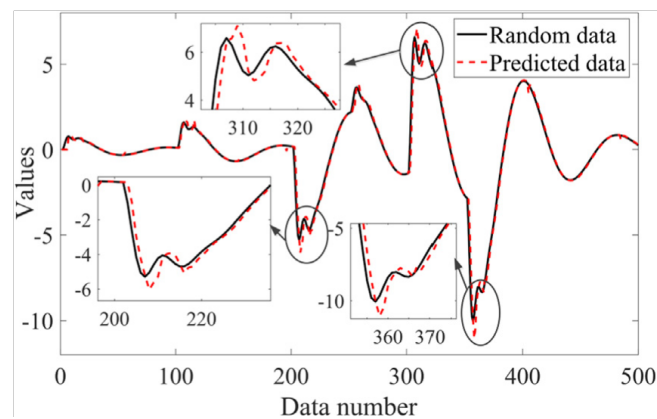
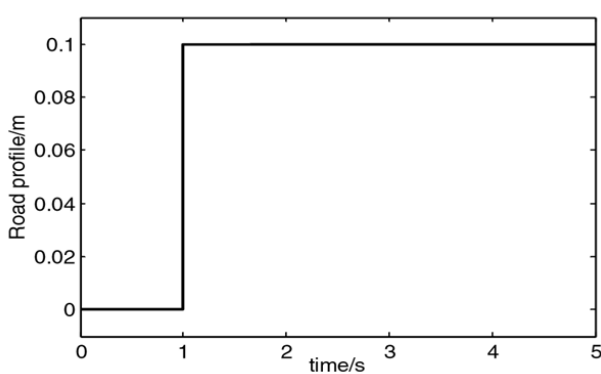
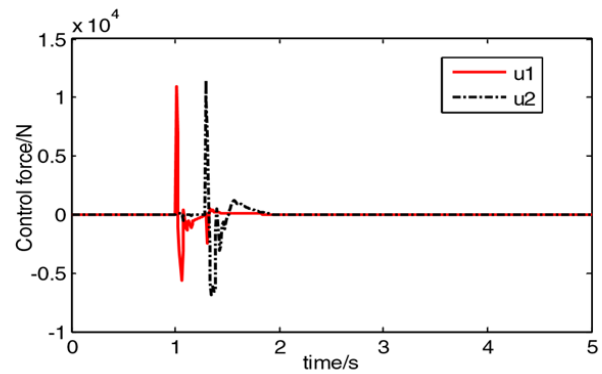


Figure 7: A numerical comparison between prediction made by DGM (2,1) model and random data.



(a) Step road profile



(b) Control signals u1 & u2

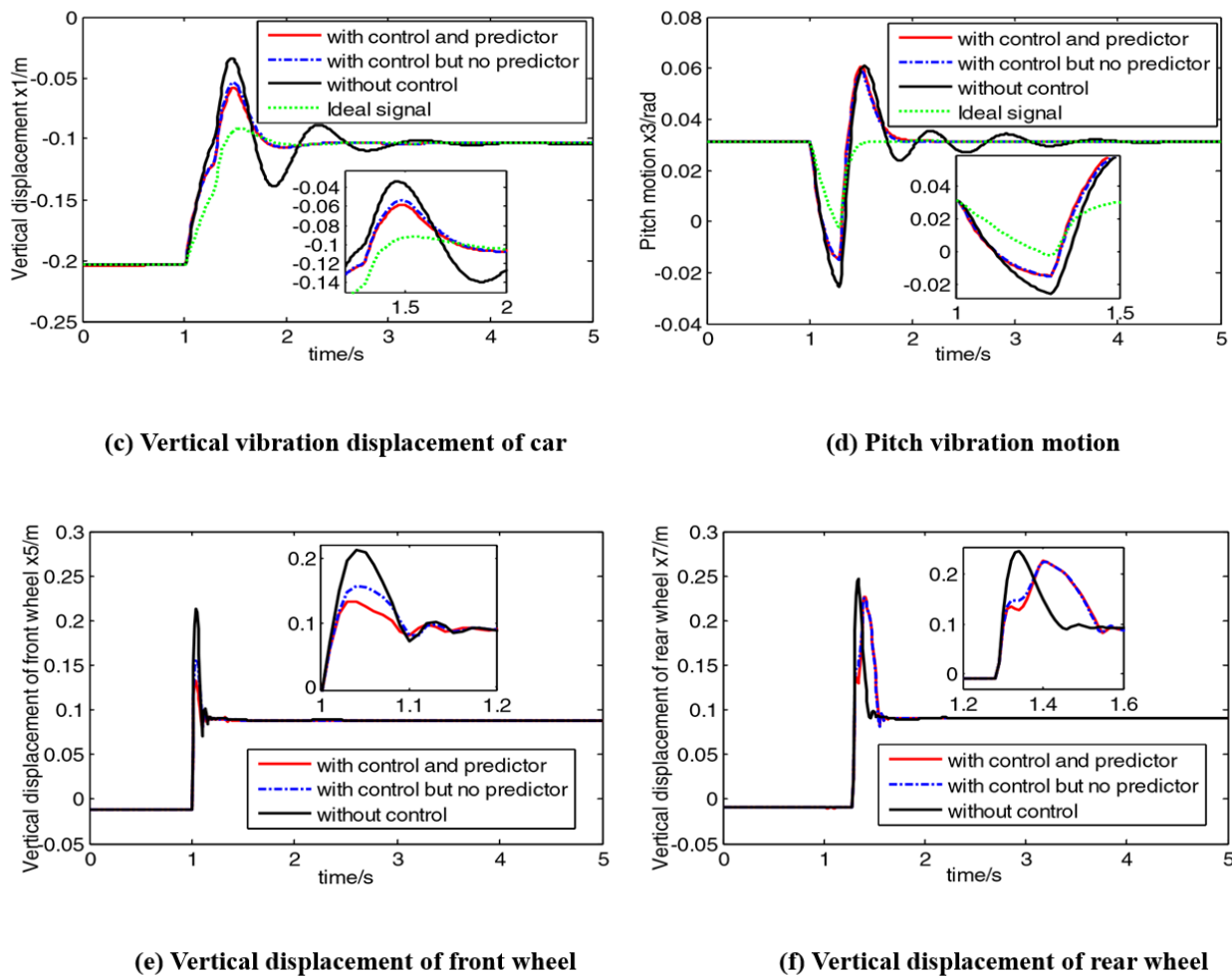


Figure 8: Vehicle suspension system control beneath the input step.

Figures 8(e) as well as 8(f) illustrate these vertical movements in the rear and front wheels under the different controls. These showed that without control, the movement of the front wheels in maximum is around 0.23 meters, while in the accustomed adaptive suppression control strategy, the movement of the front wheels in maximum is reduced to around 0.17 m which can be further reduced by 0.13 m. The vertical vibration movement in the rear wheels is decreased by 0.04 meters; however, these differences between the adaptive rear stimulus is very small without and with the signal predictor. Through the step-by-step recording, the control scheme could stabilize the car fuselage and retain the stability of the vehicle's steering. Generally, the overall performance will be better when using a gray signal predictor.

However, this limitation does not apply to the controller gain, because the overall impact of power on the entire system is relatively small. Table 3 lists all the measurable factors utilized in our EBA experiment. The actual application of EBA and its connection to the optimization problem were discussed as follows. Like other intelligent swarm algorithms and scalable schemes, EBA requires recursive operations to search the closest solution. Therefore, the same numerical experiment must be repeated several times in order to check if the numerical convergence results would be consistent. These numbers in trials which are listed in Table 3 purposefully is to furnish experimental results for a series of studies using statistical schemes.

The present study selected a fixed number in iterations as the termination condition. These materials utilized to propagate sound waves in the air because it is suitable for the natural physic environment in which the bats are located. Besides, these total sizes denote the number of people

Table 3 Measurable factor for EBA

Boundary condition for matrix positive definite matrix and controller gains	[-5, 5]
Medium Material	Air
Number of Run	40
Population size	26
Number of Iteration	700

in the solution area at the same time in each iteration. The larger the population, the greater the chances that the algorithm will find the closest solution. Yet, a large population claims more memory resources as well as computing power. Therefore, the present study fixes the population to 16 in the numerical experiment. These numbers of possible solutions implemented by EBA for numerical different varieties are indicated as seen in Figure 9.

The feedback gains and positive definite matrices with Lyapunov criterion could be referred to the existing methodology [16, 17, 18, 19]. The solutions searched by the EBA have been decided as feasible if the eigen values in Equation (9) are negative in all, the negative eigen values result in keeping stable for the large the control simulation system. Therefore, Table 4 indicates 10 numerical samples from feasible overall solutions searched by the EBA with the relevant eigen values.

Table 4 Samples in the acquired feasible numerical solutions by EBA with control system eigen values

	Matrices P and K	Eigen Values	
		with A_1, B_1	with A_2, B_2
Set 1	$P = \begin{bmatrix} 3.2641 & 0.6081 \\ 0.6081 & 0.9971 \end{bmatrix}, K^T = \begin{bmatrix} -1.4172 \\ -0.1151 \end{bmatrix}$	$\begin{bmatrix} -8.1912 \\ -2.1826 \end{bmatrix}$	$\begin{bmatrix} -9.2384 \\ -1.7674 \end{bmatrix}$
Set 2	$P = \begin{bmatrix} 3.8752 & 0.3773 \\ 0.3773 & 1.0645 \end{bmatrix}, K^T = \begin{bmatrix} -1.6726 \\ -0.2747 \end{bmatrix}$	$\begin{bmatrix} -12.9525 \\ -1.6175 \end{bmatrix}$	$\begin{bmatrix} -7.6539 \\ -1.9006 \end{bmatrix}$
Set 3	$P = \begin{bmatrix} 3.9862 & 0.6328 \\ 0.6328 & 0.3880 \end{bmatrix}, K^T = \begin{bmatrix} -1.6705 \\ -0.2633 \end{bmatrix}$	$\begin{bmatrix} -9.1133 \\ -1.9422 \end{bmatrix}$	$\begin{bmatrix} -6.5002 \\ -1.0776 \end{bmatrix}$
Set 4	$P = \begin{bmatrix} 3.4095 & 0.3250 \\ 0.3250 & 0.5086 \end{bmatrix}, K^T = \begin{bmatrix} -1.4341 \\ -0.0744 \end{bmatrix}$	$\begin{bmatrix} -2.9977 \\ -2.0886 \end{bmatrix}$	$\begin{bmatrix} -3.3554 \\ -2.3777 \end{bmatrix}$
Set 5	$P = \begin{bmatrix} 4.6075 & 0.6311 \\ 0.6311 & 0.7700 \end{bmatrix}, K^T = \begin{bmatrix} -1.4033 \\ -0.3754 \end{bmatrix}$	$\begin{bmatrix} -9.0082 \\ -3.9219 \end{bmatrix}$	$\begin{bmatrix} -6.8969 \\ -2.9625 \end{bmatrix}$
Set 6	$P = \begin{bmatrix} 4.4938 & 0.6361 \\ 0.6361 & 1.4047 \end{bmatrix}, K^T = \begin{bmatrix} -1.4631 \\ -0.7790 \end{bmatrix}$	$\begin{bmatrix} -29.3484 \\ -3.0169 \end{bmatrix}$	$\begin{bmatrix} -11.5857 \\ -2.2598 \end{bmatrix}$
Set 7	$P = \begin{bmatrix} 3.0719 & 0.0864 \\ 0.0864 & 0.9208 \end{bmatrix}, K^T = \begin{bmatrix} -1.4645 \\ -1.9464 \end{bmatrix}$	$\begin{bmatrix} -39.6258 \\ -0.5657 \end{bmatrix}$	$\begin{bmatrix} -6.3168 \\ -0.2100 \end{bmatrix}$
Set 8	$P = \begin{bmatrix} 2.7318 & 0.2748 \\ 0.2748 & 0.3832 \end{bmatrix}, K^T = \begin{bmatrix} -1.3799 \\ -1.4559 \end{bmatrix}$	$\begin{bmatrix} -13.1626 \\ -1.1711 \end{bmatrix}$	$\begin{bmatrix} -2.8163 \\ -1.8329 \end{bmatrix}$
Set 9	$P = \begin{bmatrix} 2.1372 & 0.4420 \\ 0.4420 & 0.3884 \end{bmatrix}, K^T = \begin{bmatrix} -1.7609 \\ -0.9665 \end{bmatrix}$	$\begin{bmatrix} -13.6180 \\ -1.4539 \end{bmatrix}$	$\begin{bmatrix} -4.9761 \\ -1.0774 \end{bmatrix}$
Set 10	$P = \begin{bmatrix} 1.9452 & 0.1138 \\ 0.1138 & 0.4373 \end{bmatrix}, K^T = \begin{bmatrix} -1.3655 \\ 0.0301 \end{bmatrix}$	$\begin{bmatrix} -1.2705 \\ -0.8623 \end{bmatrix}$	$\begin{bmatrix} -2.6596 \\ -0.8972 \end{bmatrix}$

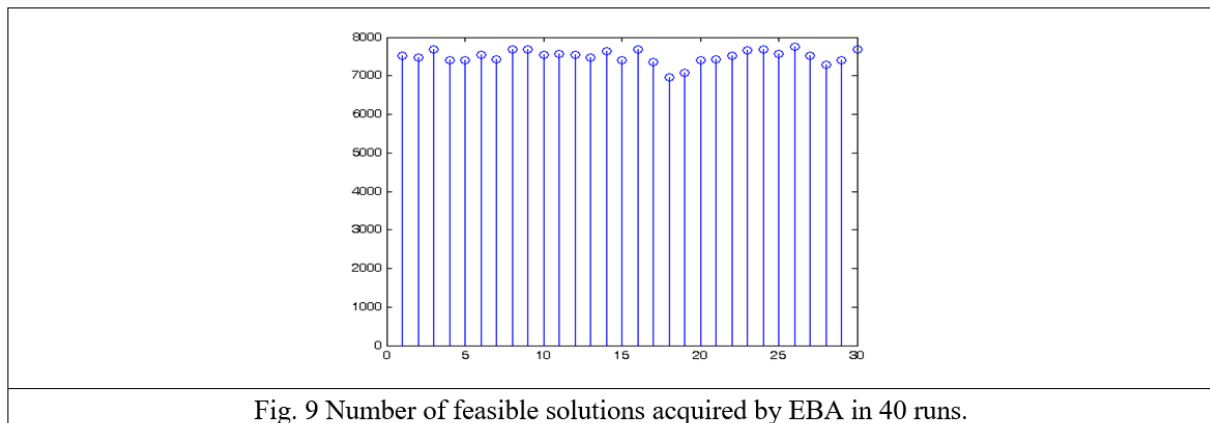


Fig. 9 Number of feasible solutions acquired by EBA in 40 runs.

5 Conclusion

This research proposes an active chassis control strategy for MEVW to enhance these driving comforts in the vehicle and limit these movements in the vehicle body during driving on the road. The theoretical basis for active vehicle suspension systems suitable for MEVW has been established. First, a nonlinear mechanical model of MEVW is established through experimental procedures. In this case, these nonlinear characteristics in the active vehicle suspension were evaluated at the same time, as well as these half-car models were accomplished. According to the Lyapunov's theory, a control law is derived to appraise the damping and stiffness in the measurable factors and track the ideal suspension. Then an hybrid improved attenuation control formula is put forward to ensure the suitable signal acquired via the control law. The feasibility and stability in the system are certificated by the Lyapunov-type theorem. In addition, a gray DGM model (2.1) is implemented in the controls to predict the movement of the vehicle suspension in advance. The simulation results represent that the formula could asymptotically stabilize the discrete-time nonlinear system through synthetic opacity control. In seeking control system solutions, the benefits of EBA model also brings flexibility and feasibility.

Compliance with Ethical Standards

The author states that there are no conflicts in interest while regarding the publication for this paper. All analyzed data and measurements during the present study are included in the article.

Funding

The author(s) received no specific funding for this work.

Author contributions

The authors contributed equally to this work.

Conflict of interest

The authors declare no conflict of interest.

References

- [1] Wang, Q.; Rajashekara, k.; Jia, Y.; Sun, J. (2017). Multiple quantile regression analyses of longitudinal data: heteroscedasticity and efficient estimation, *IEEE Transactions on Vehicle Technologies*, 66(9), 2017, 7722-7729.
- [2] Pfluger, J.; Savelsberg, R.; Hülshorst, T.; Pischinger, S., & Andert, J. (2018). Potential of Real-Time Cylinder Pressure Analysis by Using Field Programmable Gate Arrays, *International Journal of Automotive Technology*, 19, 643-650.
- [3] Silva, G. J.; Datta, A.; Bhattacharyya, S. P. (2002). New results on the synthesis of PID controllers, *IEEE Transactions on Automation Control*, 47(2), 241-252, Aug. 2002.
- [4] Chen, T.; Kuo, D.; Chen, C. Y. J. (2021a). Fuzzy C-means robust algorithm for nonlinear systems, *Soft Computing*, 25(11), 7297-7305.
- [5] Chen, T.; Huang, Y. C.; Chen, C. Y. J. (2021b). Smart structural stability and NN based intelligent control for nonlinear systems, *Smart Structures and Systems*, 27.
- [6] Chen, T.; Huang, Y. C.; Chen, C. Y. J. (2021c). Wind vibration control of stay cables using an evolutionary algorithm, *Wind and Structures*, 32(1), 73-86.
- [7] Jiang, Y.; Yang, C.; Ma, H. (2016). A Review of Fuzzy Logic and Neural Network Based Intelligent Control Design for Discrete-Time Systems, *Discrete Dynamics in Nature and Society*, 2016, 1-11.
- [8] Wang, T.; Sui, S.; Tong, S. (2017). Data-based adaptive neural network optimal output feedback control for nonlinear systems with actuator saturation, *Neurocomputing*, 247, 192-201.
- [9] Kaur, R.; Jyoti, Navjot. (2016). Image Segmentation using Hybrid Particle Swarm Optimization & Penalized Fuzzy C-Mean Clustering, *International Journal of Engineering Research and General Science*, 4(1), 256-261, 2091-2730, 2016.
- [10] Feng, H. H.; Feng, H.; Horng, J.; Jou, S. (2012). Bacterial Foraging Particle Swarm Optimization Algorithm Based Fuzzy-VQ Compression Systems, *Journal of Information Hiding and Multimedia Signal Processing*, 3, 227-239.
- [11] Li, R. J.; Lee, E. S. (1989). Analysis of Fuzzy Queues, *Computers and Mathematics with Applications*, 17(7), 1143-1147.
- [12] Chen, T.; Chen, C. Y. J. (2021). Optimized AI controller for reinforced concrete frame structures under earthquake excitation, *Advances in Concrete Construction*, 11(1), 1-9, 2021
- [13] Kazemian, A. H.; Fooladi, M.; Darijani, H. (2019). Non-linear control of vehicle's rollover using sliding mode controller for new 8 degrees of freedom suspension model, *International Journal of Heavy Vehicle Systems*, 26, 707.
- [14] Latrech, C.; Kchaou, M.; Guéguen, H. (2018). Networked non-fragile H_∞ static output feedback control design for vehicle dynamics stability: A descriptor approach, *European Journal of Control*, 40, 13-26.
- [15] Li, W.; Xie, Z.; Wong, P.; Ma, X.; Cao, Y.; Zhao, J. (2019). Nonfragile H_∞ Control of Delayed Active Suspension Systems in Finite Frequency Under Nonstationary Running, *Journal of Dynamic Systems Measurement and Control-transactions of The Asme*, 141, 061001.
- [16] Chen, T.; Rao, S.; Sabitovich, R. T.; Chapron, B.; Chen, C. Y. J. (2020). An Intelligent Algorithm Optimum for Building Design of Fuzzy Structures, *Iranian Journal of Science and Technology, Transactions of Civil Engineering*, 44, 523-531, 2020.
- [17] Chen, T.; Khurram, S.; Pandey, L.; Chen, J. C. Y. (2020). LMI based criterion for reinforced concrete frame structures, *Advances in Concrete Construction*, 9(4), 407-412.

- [18] Chen, T.; Babanin, A.; Muhammad, A.; Chapron, B., Chen, C. Y. J. (2020). Evolved fuzzy NN control for discrete-time nonlinear systems based on fuzzy Lyapunov methods, *Journal of Circuits, Systems and Computers*, 29(1), 2050015.
- [19] Chen, C. W. (2014). A criterion of robustness intelligent nonlinear control for multiple time-delay systems based on fuzzy Lyapunov methods, *Nonlinear Dynamics*, 76, 23-31.
- [20] Xia, X.; Liu, P.; Zhang, N.; Ning, D.; Zheng, M.; Du, H. (2019). Takagi-Sugeno Fuzzy Control for the Semi-active Seat Suspension with an Electromagnetic Damper, *3rd Conference on Vehicle Control and Intelligence (CVCI)*, 1-6.
- [21] Chatterjee, A.; Chatterjee, R. (2008). Augmented Stable Fuzzy Control for Flexible Robotic Arm Using LMI Approach and Neuro-Fuzzy State Space Modeling, *IEEE Transactions On Industrial Electronics*, 55(3), 3671-3681, March 2008.
- [22] Haidegger, T.; Kovács, L.; Precup, R. E.; Preitl, S.; Benyó, B.; Benyó, Z. (2011). Cascade control for telerobotic systems serving space medicine, *IFAC Proceedings Volumes*, 44(1), 3759-3764, January 2011.
- [23] Precup, R. E.; Tomescu, M. L. (2015). Stable fuzzy logic control of a general class of chaotic systems, *Neural Computing and Applications*, 26(3), 541-550, 2015.
- [24] Sun, W.; Gao, H.; Kaynak, O. (2013). Adaptive backstepping control for active suspension systems with hard constraints, *IEEE/ASME Transactions on Mechatronics*, 18(3), 1072-1079, 2013.
- [25] Zhao, Y.; Deng, Y.; Lin, F.; Zhu, M.; Xiao, Z. (2018). Transient Dynamic Characteristics of a Non-Pneumatic Mechanical Elastic Wheel Rolling Over a Ditch, *International Journal of Automotive Technology*, 19, 499-508.
- [26] Dzitac, I.; Filip, F. G.; Manolescu, M. J. (2017). Fuzzy logic is not fuzzy: World-renowned computer scientist Lotfi A. Zadeh, *International Journal of Computers Communications & Control*, 12(6), 748-789, 2017.
- [27] Khosravi, A.; Nahavandi, S.; Creighton, D.; Srinivasan, D. (2012). Interval type-2 fuzzy logic systems for load forecasting: A comparative study, *IEEE Transactions on Power Systems*, 27(3), 1274-1282, 2012.
- [28] Liang, Q.; Mendel, J. M. (1999). An introduction to type-2 TSK fuzzy logic systems, *IEEE International Fuzzy Systems*, Conference Proceedings (Cat. No. 99CH36315), IEEE, 1999.
- [29] Haidegger, T.; Kovács, L.; Preitl, S.; Precup, R. E.; Benyo, B.; Benyo, Z.; Controller design solutions for long distance telesurgical applications, *International Journal of Artificial Intelligence*, 6(11), 48-71, March 2011.
- [30] Yu, J.; Zhang, K.; Fei, S. (2008). Adaptive Fuzzy Tracking Control of a Class of Stochastic Nonlinear Systems with Unknown Dead-Zone Input, *International Journal of Fuzzy Systems*, 10, 18-23.
- [31] Li, H.; Jing, X.; Lam, H.; Shi, P. (2014). Fuzzy sampled-data control for uncertain, *IEEE Transactions on Cybernetics*, 44(7), 1111-1126, 2014.
- [32] Li, H.; Jing, X.; Karimi, H. R. (2014). Output-Feedback-Based H_∞ Control for Vehicle Suspension Systems With Control Delay, *IEEE Transactions on Industrial Electronics*, 61(1), 436-446, 2014.
- [33] Yu, E.; Ambati, A.; Andersen, M. S.; Krohn, L.; Estiar, M. A.; Saini, P.; Senkevich, K.; Sosero, Y. L.; Sreelatha, A. A.; Ruskey, J.; Asayesh, F.; Spiegelman, D.; Toft, M.; Viken, M. K.; Con, T. I.; Sharma, M.; Blauwendraat, C.; Pihlstrøm, L.; Mignot, E.; Gan-Or, Z. (2020). Fine mapping of the HLA locus in Parkinson's disease in Europeans, *medRxiv*, November 03, 2020.

- [34] Wu, F.; Chang, G.; Deng, K.; Tao, W. (2019). Selecting data for autoregressive modeling in polar motion prediction, *Acta Geodaetica et Geophysica*, 54(4), 557-566.
- [35] Shao, Y.; Wei, Y.; Su, H. (2010). On Approximating Grey Model DGM(2,1), *Journal of Grey Systems: Elsevier*, 22(4), 333-340, 2010.
- [36] Li, K.; Zhang, T. (2018). Forecasting Electricity Consumption Using an Improved Grey Prediction Model, *Information: MDPI*, 9(8), 204, 2018.
- [37] Chen, C. W. (2014). Interconnected TS fuzzy technique for nonlinear time-delay structural systems, *Nonlinear Dynamics*, 76, 13-22, 2014.
- [38] Tsai, P. W.; Pan, J. S.; Liao, B. Y.; Tsai, M. J.; Vaci, I. (2012). Bat Algorithm Inspired Algorithm for Solving Numerical Optimization Problems, *Applied Mechanics and Materials*, 148-149, 134-137, 2012.
- [39] Tsai, P. W.; Chen, C. W. (2014). A Novel Criterion for Nonlinear Time-Delay Systems Using LMI Fuzzy Lyapunov Method, *Applied Soft Computing*, 25, 461-472.
- [40] Tsai, P. W.; Alsaedi, A.; Hayat, T.; Chen, C. W. (2016). A Novel Control Algorithm for Interaction between Surface Waves and a Permeable Floating Structure, *China Ocean Engineering*, 30(2), 161-176.
- [41] Chen, T.; Chen, J. C. Y. (2020). On the algorithmic stability of optimal control with derivative operators, *Circuits Systems and Signal Process*, 39, 5863-5881, 2020.
- [42] Chen, T.; Crosbie, R. C.; Anandkumarb, A.; Melville, C.; Chan, J. (2021). Optimized AI controller for reinforced concrete frame structures under earthquake excitation, *Advances in Concrete Construction*, 11(1), 1-9, January 2021.

Appendix

Let the Lyapunov function in the nonlinear system be expounded as

$$V(k) = x(k)^T P x(k) \tag{A.1}$$

where P is a positive definite matrix. We thus appraise the backward difference in V(k) on the trajectories to get

$$\begin{aligned} \Delta V(k) &= -V(k) + V(k+1) = \mathbf{x}(k+1)^T \mathbf{P} \mathbf{x}(k+1) - \mathbf{x}(k)^T \mathbf{P} \mathbf{x}(k) \\ &= \left\{ \sum_{i=1}^{\phi} \sum_{j=1}^l h_i(k) \bar{h}_j(k) \mathbf{H}_{ij} \mathbf{x}(k) + \mathbf{e}(k) \right\}^T \mathbf{P} \left\{ \sum_{i=1}^{\phi} \sum_{j=1}^l h_i(k) \bar{h}_j(k) \mathbf{H}_{ij} \mathbf{x}(k) + \mathbf{e}(k) \right\} - \mathbf{x}(k)^T \mathbf{P} \mathbf{x}(k) \end{aligned} \tag{A.2}$$

Let

$$\sum_{i=1}^{\phi} \sum_{j=1}^l \sum_{\alpha=1}^{\phi} \sum_{\beta=1}^l h_i(k) \bar{h}_j(k) h_{\alpha}(k) \bar{h}_{\beta}(k) \mathbf{x}(k)^T \{ \mathbf{H}_{ij}^T \mathbf{P} \mathbf{H}_{\alpha\beta} - \mathbf{P} \} \mathbf{x}(k) = m_1 + m_2 + m_3 + m_4 \tag{A.3}$$

Where,

$$\begin{aligned}
 m_1 &\equiv \sum_{i=\alpha}^{\phi} \sum_{j=\beta}^l h_i^2(k) \bar{h}_j^2(k) \mathbf{x}(k)^T (\mathbf{H}_{ij}^T \mathbf{P} \mathbf{H}_{ij} - \mathbf{P}) \mathbf{x}(k), \\
 m_2 &\equiv \sum_{i \neq \alpha}^{\phi} \sum_{j=\beta}^l h_i(k) h_{\alpha}(k) \bar{h}_j^2(k) \mathbf{x}(k)^T (\mathbf{H}_{ij}^T \mathbf{P} \mathbf{H}_{\alpha j} - \mathbf{P}) \mathbf{x}(k) \\
 &= \sum_{i < \alpha}^{\phi} \sum_{j=\beta}^l h_i(k) h_{\alpha}(k) \bar{h}_j^2(k) \mathbf{x}(k)^T \{ \mathbf{H}_{ij}^T \mathbf{P} \mathbf{H}_{\alpha j} + \mathbf{H}_{\alpha j}^T \mathbf{P} \mathbf{H}_{ij} - 2\mathbf{P} \} \mathbf{x}(k), \\
 m_3 &\equiv \sum_{i=\alpha}^{\phi} \sum_{j \neq \beta}^l h_i^2(k) \bar{h}_j(k) \bar{h}_{\beta}(k) \mathbf{x}(k)^T (\mathbf{H}_{ij}^T \mathbf{P} \mathbf{H}_{i\beta} - \mathbf{P}) \mathbf{x}(k) \\
 &= \sum_{i=\alpha}^{\phi} \sum_{j < \beta}^l h_i^2(k) h_j(k) h_{\beta}(k) \mathbf{x}(k)^T \{ \mathbf{H}_{ij}^T \mathbf{P} \mathbf{H}_{i\beta} + \mathbf{H}_{i\beta}^T \mathbf{P} \mathbf{H}_{ij} - 2\mathbf{P} \} \mathbf{x}(k), \\
 m_4 &\equiv \sum_{i \neq \alpha}^{\phi} \sum_{j \neq \beta}^l h_i(k) \bar{h}_j(k) h_{\alpha}(k) \bar{h}_{\beta}(k) \mathbf{x}(k)^T (\mathbf{H}_{ij}^T \mathbf{P} \mathbf{H}_{\alpha\beta} - \mathbf{P}) \mathbf{x}(k) \\
 &= \sum_{i < \alpha}^{\phi} \sum_{j < \beta}^l h_i(k) h_{\alpha}(k) h_j(k) h_{\beta}(k) \mathbf{x}(k)^T \{ \mathbf{H}_{ij}^T \mathbf{P} \mathbf{H}_{\alpha\beta} + \mathbf{H}_{\alpha\beta}^T \mathbf{P} \mathbf{H}_{ij} - 2\mathbf{P} \} \mathbf{x}(k).
 \end{aligned}$$

Therefore, we have

$$\begin{aligned}
 m_2 &= \sum_{i < \alpha}^{\phi} \sum_{j=\beta}^l h_{\alpha}(k) h_i(k) \bar{h}_j^2(k) \mathbf{x}(k)^T \{ -[\mathbf{H}_{ij} - \mathbf{H}_{\alpha j}]^T \mathbf{P} [\mathbf{H}_{ij} - \mathbf{H}_{\alpha j}] + \mathbf{H}_{ij}^T \mathbf{P} \mathbf{H}_{ij} - \mathbf{P} \\
 &\quad + \mathbf{H}_{\alpha j}^T \mathbf{P} \mathbf{H}_{\alpha j} - \mathbf{P} \} \mathbf{x}(k) < 0 \quad \text{for } j = \beta = 1, \dots, l; i < \alpha \leq \phi.
 \end{aligned} \tag{A.4}$$

For the similar phase

$$m_3 < 0 \text{ and } m_4 < 0 \tag{A.5}$$

Substituting (A.4) and (A.5) into (A.3) yields

$$\begin{aligned}
 &\sum_{i=1}^{\phi} \sum_{j=1}^l \sum_{\alpha=1}^{\phi} \sum_{\beta=1}^l \bar{h}_j(k) h_i(k) \bar{h}_{\beta}(k) h_{\alpha}(k) \mathbf{x}(k)^T \{ \mathbf{H}_{ij}^T \mathbf{P} \mathbf{H}_{\alpha\beta} - \mathbf{P} \} \mathbf{x}(k) \\
 &\leq \sum_{i=1}^{\phi} \sum_{j=1}^l \bar{h}_j(k) h_i(k) \mathbf{x}(k)^T (\mathbf{H}_{ij}^T \mathbf{P} \mathbf{H}_{ij} - \mathbf{P}) \mathbf{x}(k).
 \end{aligned} \tag{A.6}$$

From (A.6) and (A.2), we have

$$\begin{aligned}
 \Delta V(k) &\leq \sum_{i=1}^{\phi} \sum_{j=1}^l \bar{h}_j(k) h_i(k) \mathbf{x}(k)^T (\mathbf{H}_{ij}^T \mathbf{P} \mathbf{H}_{ij} - \mathbf{P}) \mathbf{x}(k) \\
 &\quad + \sum_{i=1}^{\phi} \sum_{j=1}^l \bar{h}_j(k) h_i(k) \{ \mathbf{x}(k)^T \mathbf{H}_{ij}^T \mathbf{P} \mathbf{e}(k) + \mathbf{e}(k)^T \mathbf{P} \mathbf{H}_{ij} \mathbf{x}(k) \} + \mathbf{e}(k)^T \mathbf{P} \mathbf{e}(k).
 \end{aligned} \tag{A.7}$$

Since P belongs to positive definite matrix, then it derives that

$$\begin{aligned}
 &(\kappa^2 \mathbf{H}_{ij} \mathbf{x}(k) - \kappa^{-2} \mathbf{e}(k))^T \mathbf{P} (\kappa^2 \mathbf{H}_{ij} \mathbf{x}(k) - \kappa^{-2} \mathbf{e}(k)) \geq 0 \\
 &\Rightarrow \kappa \mathbf{x}(k)^T \mathbf{H}_{ij}^T \mathbf{P} \mathbf{H}_{ij} \mathbf{x}(k) - \mathbf{x}(k)^T \mathbf{H}_{ij}^T \mathbf{P} \mathbf{e}(k) - \mathbf{e}(k)^T \mathbf{P} \mathbf{H}_{ij} \mathbf{x}(k) + \kappa^{-1} \mathbf{e}(k)^T \mathbf{P} \mathbf{e}(k) \geq 0 \\
 &\Rightarrow \mathbf{x}(k)^T \mathbf{H}_{ij}^T \mathbf{P} \mathbf{e}(k) + \mathbf{e}(k)^T \mathbf{P} \mathbf{H}_{ij} \mathbf{x}(k) \leq \kappa \mathbf{x}(k)^T \mathbf{H}_{ij}^T \mathbf{P} \mathbf{H}_{ij} \mathbf{x}(k) + \kappa^{-1} \mathbf{e}(k)^T \mathbf{P} \mathbf{e}(k).
 \end{aligned}$$

Therefore, we acquire

$$\begin{aligned}
 \Delta V(k) &\leq \sum_{i=1}^{\varphi} \sum_{j=1}^l \bar{h}_j(k) h_i(k) \mathbf{x}(k)^T \{ \mathbf{H}_{ij}^T \mathbf{P} \mathbf{H}_{ij} - \mathbf{P} \} \mathbf{x}(k) \\
 &\quad + \sum_{i=1}^{\varphi} \sum_{j=1}^l \bar{h}_j(k) h_i(k) \{ \kappa \mathbf{x}(k)^T \mathbf{H}_{ij}^T \mathbf{P} \mathbf{H}_{ij} \mathbf{x}(k) \} + (1 + \kappa^{-1}) \mathbf{e}(k)^T \mathbf{P} \mathbf{e}(k) \\
 &= \sum_{i=1}^{\varphi} \sum_{j=1}^l \bar{h}_j(k) h_i(k) \mathbf{x}(k)^T \{ (1 + \kappa) \mathbf{H}_{ij}^T \mathbf{P} \mathbf{H}_{ij} - \mathbf{P} \} \mathbf{x}(k) + (1 + \kappa^{-1}) \mathbf{e}(k)^T \mathbf{P} \mathbf{e}(k) \\
 &\leq \sum_{i=1}^{\varphi} \sum_{j=1}^l \bar{h}_j(k) h_i(k) \mathbf{x}(k)^T \{ (1 + \kappa) \mathbf{H}_{ij}^T \mathbf{P} \mathbf{H}_{ij} - \mathbf{P} \} \mathbf{x}(k) + (1 + \kappa^{-1}) \lambda_{\max}(\mathbf{P}) \mathbf{e}(k)^T \mathbf{e}(k).
 \end{aligned}
 \tag{A.8}$$

From (A.8) we can get

$$\Delta V(k) \leq \sum_{i=1}^{\varphi} \sum_{j=1}^l \bar{h}_j(k) h_i(k) \mathbf{x}(k)^T \{ (1 + \kappa) \mathbf{H}_{ij}^T \mathbf{P} \mathbf{H}_{ij} - \mathbf{P} + (1 + \kappa^{-1}) \lambda_{\max}(\mathbf{P}) \mathbf{H}_q^T \mathbf{H}_q \} \mathbf{x}(k).
 \tag{A.9}$$

The nonlinear closed-loop system is asymptotically vibration stable.



Copyright ©2021 by the authors. Licensee Agora University, Oradea, Romania.

This is an open access article distributed under the terms and conditions of the Creative Commons Attribution-NonCommercial 4.0 International License.

Journal’s webpage: <http://univagora.ro/jour/index.php/ijccc/>



This journal is a member of, and subscribes to the principles of, the Committee on Publication Ethics (COPE).

<https://publicationethics.org/members/international-journal-computers-communications-and-control>

Cite this paper as:

Chen, T.; Hung, C. C.; Huang, Y. C.; Chen, J. C. Y; Rahman, Md. S.; Mozumder, Md. T. I. (2021). Grey signal predictor and fuzzy controls for active vehicle suspension systems via Lyapunov theory, *International Journal of Computers Communications & Control*, 16(3), 3991, 2021.

<https://doi.org/10.15837/ijccc.2021.3.3991>